TABLE OF CONTENTS

BIOMED BASIC SCIENCE

Increased cutaneous bacterial load of immunosuppressed organ transplant recipients

Burhan A. Khan[1], Priyamvada Sobarun[1,3], Sharon Gavizon[3], Nancy Lachner[2], Li Lin[1], Mark Morrison[1], Philip Hugenholtz[2], Ian H. Frazer[1], H. Peter Soyer[1,3]

[1] Diamantina Institute, University of Queensland; Brisbane, QLD, Australia

[2] Australian Centre for Ecogenomics, University of Queensland; St Lucia, QLD, Australia

[3] Dermatology Department, Princess Alexandra Hospital, Metro South Health; Woolloongabba, QLD, Australia

BACKGROUND

- Nonmelanoma skin cancer is the most common cancer among Caucasians and is increasing in prevalence
- Iatrogenic immunosuppression of organ transplant recipients has been associated with a higher risk of developing cutaneous squamous cell carcinoma (cSCC)
- Immunological factors are a determinant of neoplastic progression from premalignant actinic keratosis (AK) and intraepithelial carcinoma (IEC) to cSCC

METHODOLOGY

- Cross-sectional observational study
- Immunocompromised organ transplant patients (n=32) enrolled into 3 groups of increasing sun damage
- Immunocompetent control group (n=11)
- Skin swabbed:
  - Non-lesioned forearm skin (3/pt)
  - Forearm AKs (3-5/pt)
  - Suspected SCCs
- Swabs cultured on non-selective media for aerobic growth
- Diagnosis
  - AK → clinical
  - IEC & SCC → biopsy-proven

RESULTS

OTR demographics (n=32)		
Characteristic		
Average age	62 (range=44-80)	
Sex	**n**	**%**
Male	26	81.3
Female	6	18.8
Fitzgerald Skin Type		
I	7	21.9
II	20	62.5
III	4	12.5
IV	1	3.1
V	0	-
VI	0	-

Microbial load by immune status

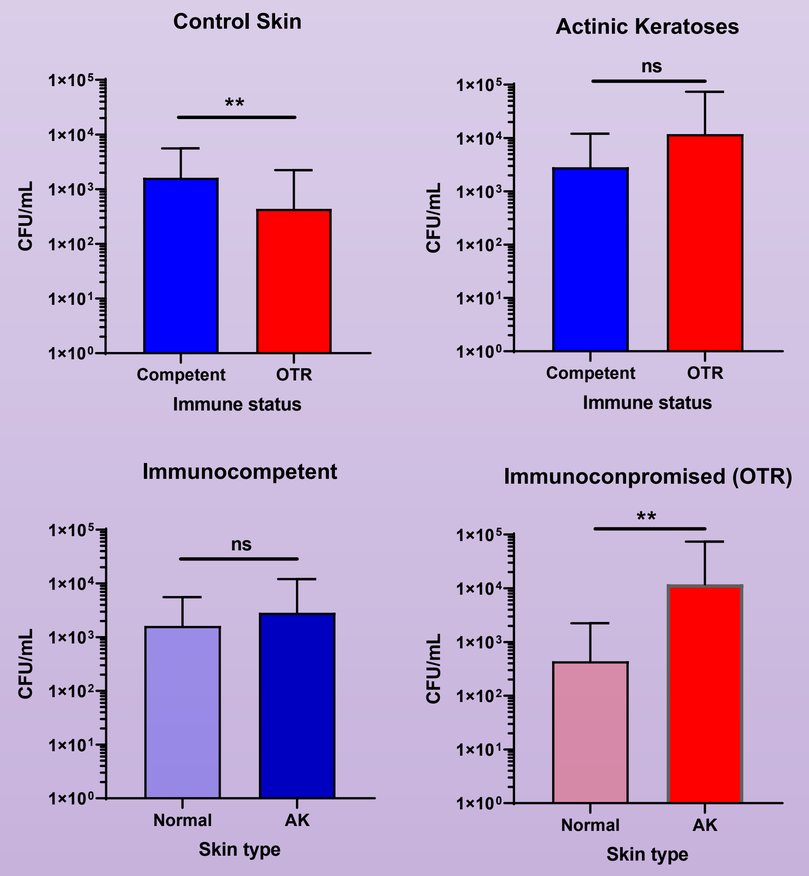

Average microbial load by OTR group

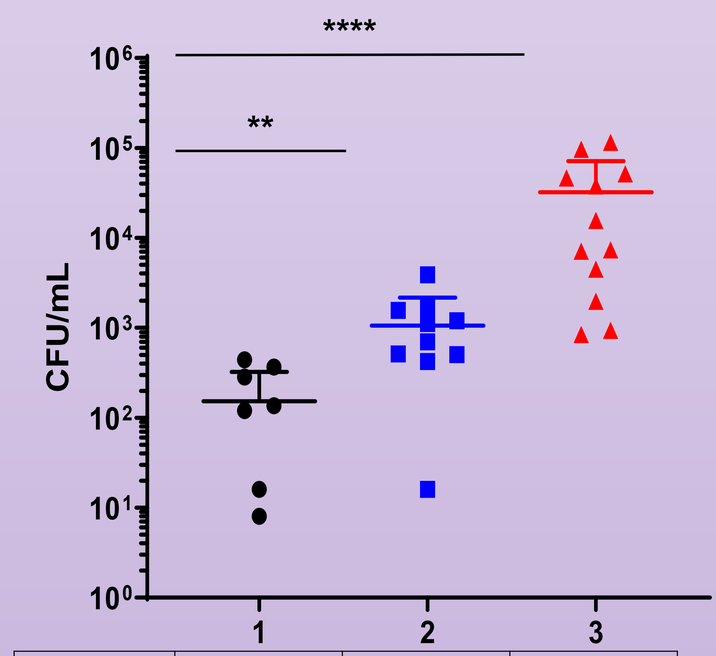

AK/IEC	-	+	+
cSCC	-	-	+

Microbial Load by OTR Lesion Type

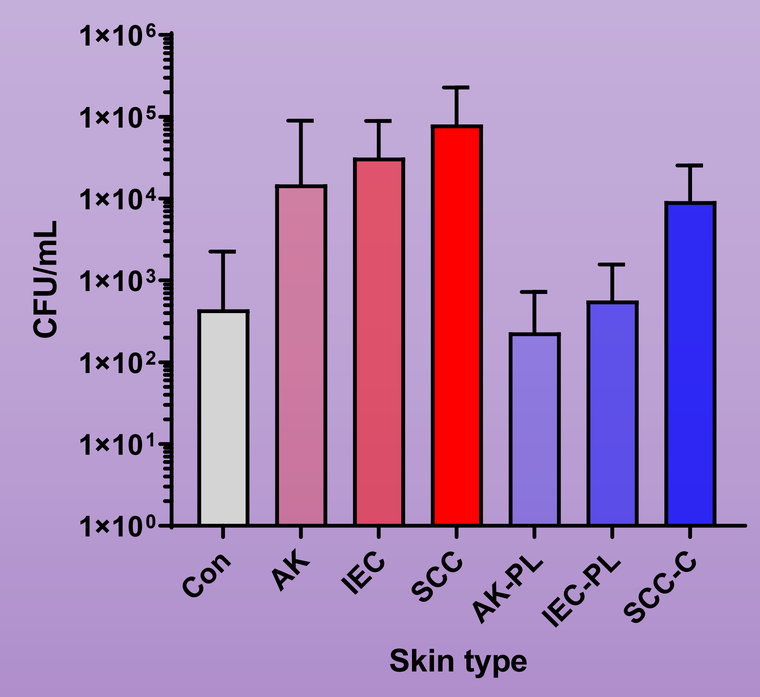

Microbial load of multiple OTR lesions

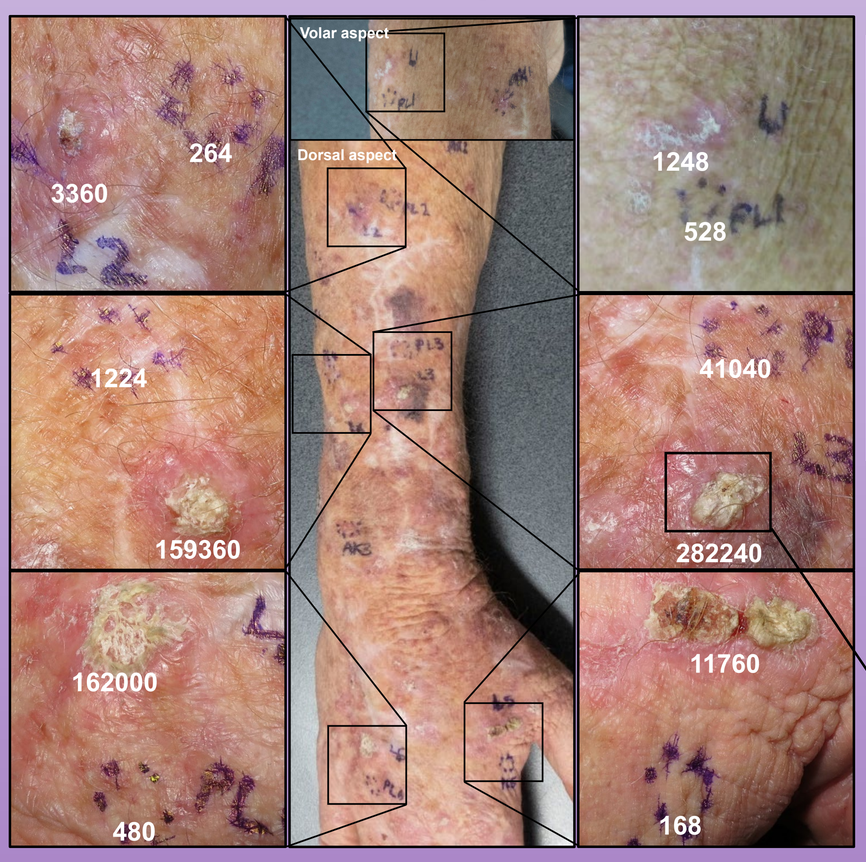

Bacteria visible in s. corneum of cSCC

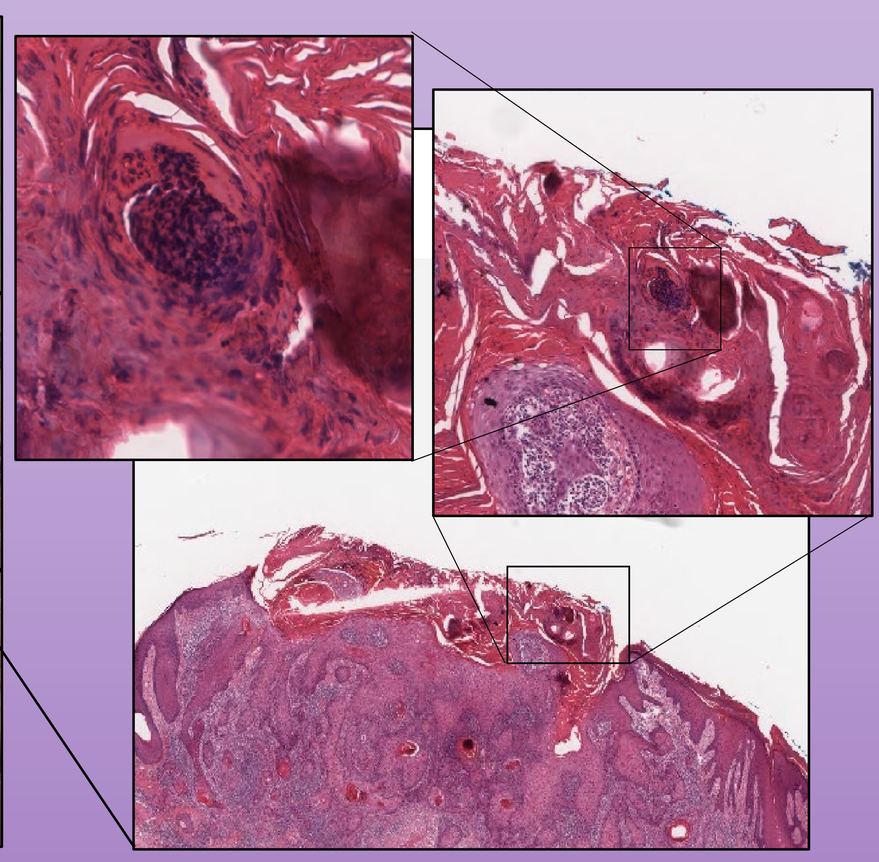

CONCLUSIONS

- Increased bacterial load on sun-damaged skin vs normal skin
- Increasing severity of epidermal dysplasia correlated with higher bacterial burden
- Immune suppression correlated with higher overall cutaneous bacterial burden

CONTACT

Burhan A. Khan, MSc
b.khan@uq.net.au
v-bukhan@ochsner.org

THE UNIVERSITY OF QUEENSLAND AUSTRALIA

Australian Centre for Ecogenomics

DIAMANTINA INSTITUTE

TRI TRANSLATIONAL RESEARCH INSTITUTE AUSTRALIA

Queensland Government

Metro South Health

Princess Alexandra Hospital

Brain-derived neurotrophic factor in cerebrospinal fluid as a potential biomarker for Huntington's disease

Zhen-Yi Andy Ou[1], Lauren M. Byrne[1], Filipe B. Rodrigues[1], Rosanna Tortelli[1], Eileanoir B. Johnson[1], Martha S. Foiani[4], Marzena Arridge[2], Enrico De Vita[2,3], Rachael I. Scahill[1], Amanda Heslegrave[4], Henrik Zetterberg[4,5,6], Edward J. Wild[1]

Introduction

Brain-derived neurotrophic factor (BDNF), a member of the neurotrophin family that maintains neuronal development, survival, and synaptic plasticity, is synthesized in the cortical neurons and transported to striatal neurons. BDNF synthesis and transport are regulated by huntingtin (HTT) protein.

In HD, it is thought that mutated HTT-induced deficit of BDNF may be involved in early selective striatal neurons vulnerability. BDNF has never been quantified in cerebrospinal fluid (CSF) as a potential biomarker for HD progression.

We aimed to investigate BDNF in plasma and CSF and their relative association with clinical and imaging measures.

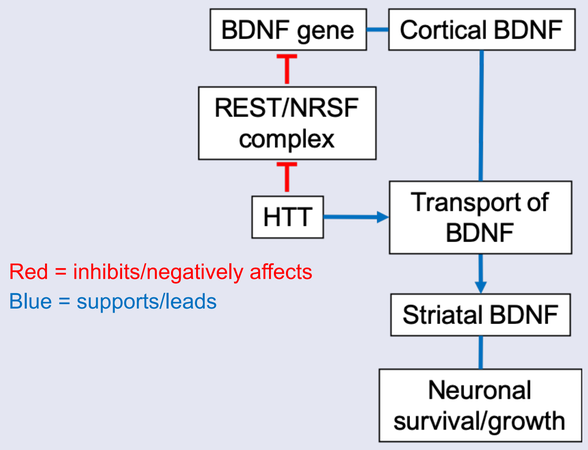

Schematic diagram of BDNF and HTT

Methods

- First, we compared several commercially available immunoassays: Human BDNF ELISA Kit (Sigma-Aldrich, Saint Louis, MO, United States), BDNF Emax ImmunoAssay System (Promega, Madison, WI, United States), and SIMOA Human BDNF Discovery Kit (Quanterix™, Lexington, MA, United States).
- Then, we employed SIMOA (single-molecule array) to quantify BDNF concentration in 20 controls, 20 premanifest HD, and 37 manifest HD.
- All analyses including multivariable linear regression and ROC analysis, were performed with Stata 15.1.

Results: ELISA versus SIMOA

- Blood BDNF was quantifiable and correlated in all three immunoassays.
- CSF BDNF was below the limit of quantification in Promega (20/20) and Sigma-Aldrich (4/20) ELISAs.
- SIMOA was able to quantify BDNF in all plasma and CSF samples.

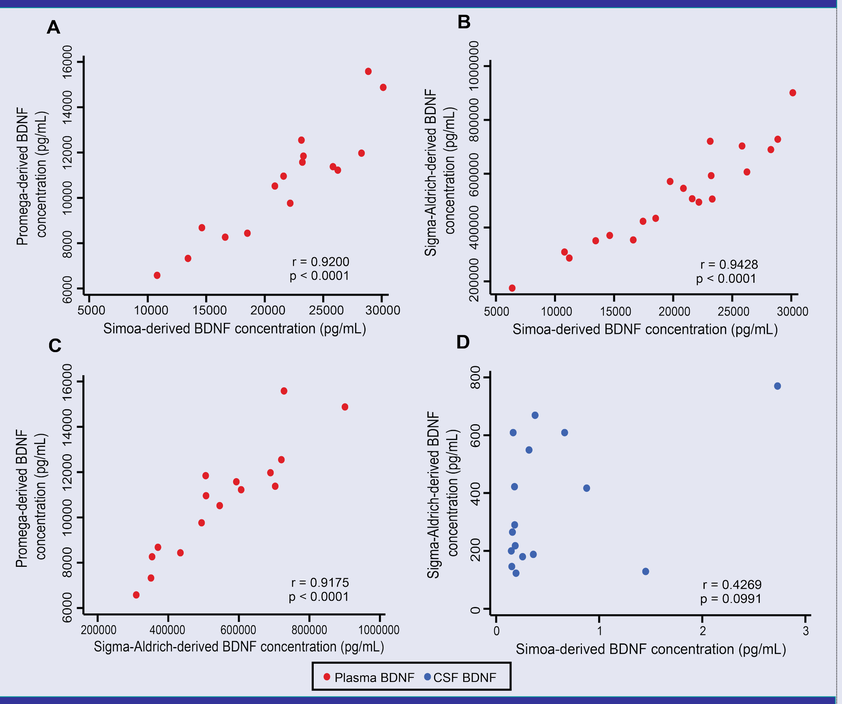

Results: BDNF level by group

Table 1. Basic characteristics of the HD-CSF cohort

	Control	Premanifest HD	Manifest HD	ANOVA (p-value)	Control vs PreHD (p-value)	PreHD vs HD (p-value)
N	20	20	37	N/A	N/A	N/A
Males *n (%)*	10 (50)	10 (50)	19 (51)	0.993	1.000	0.922
Age (years)	50.7 ± 11.0	42.4 ± 11.0	56.4 ± 9.5	**<0.0001**	**0.013**	**<0.0001**
BMI (kg/m^2)	29.0 ± 7.9	25.1 ± 3.0	24.8 ± 5.0	**0.020**	**0.027**	0.859
On medication (%)	15 (75)	15 (75)	36 (97)	**0.010**	1.000	**0.017**
CAG repeats	N/A	42.4 ± 1.6	42.7 ± 2.3	N/A	N/A	0.207
Blood platelet (10^9/L)	244 ± 49.1	231.7 ± 38.9	261.4 ± 65.4	0.148	0.491	0.058
CSF erythrocyte (per µL)	8.5 ± 27.6	3.3 ± 7.1	38.9 ± 161.5	0.443	0.884	0.262
CSF hemoglobin (ng/ml)	416.7 ± 634.2	475.9 ± 543.2	262.6 ± 243.0	0.200	0.683	0.096
Disease burden score	N/A	267.1 ± 61.9	396.4 ± 97.5	N/A	N/A	**<0.0001**

Values are presented as mean ± *SD*.

- BDNF did not differ between healthy controls and HD mutation carriers at any stages.

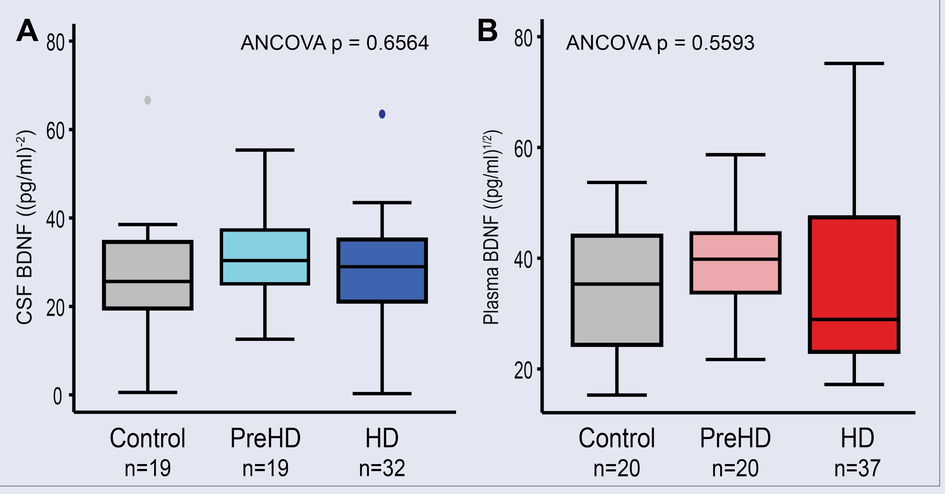

ANCOVA p-value was adjusted for age, gender, BMI, anti-depressant, anti-psychotic, and erythrocyte level in CSF.

ANCOVA p-value was adjusted for age, gender, BMI, anti-depressant, anti-psychotic, storage duration, and platelet level in blood.

Results: Clinical & imaging associations of BDNF

- BDNF level was not significantly associated with the clinical measures.

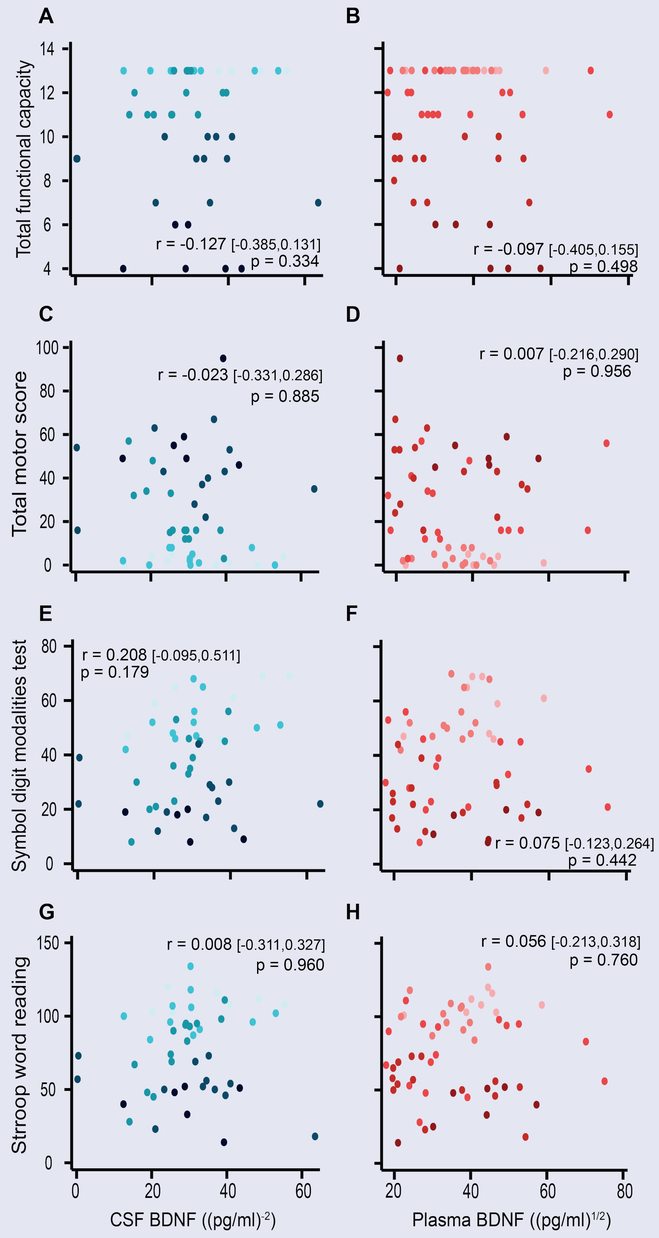

- BDNF level was not significantly associated with the imaging measures.

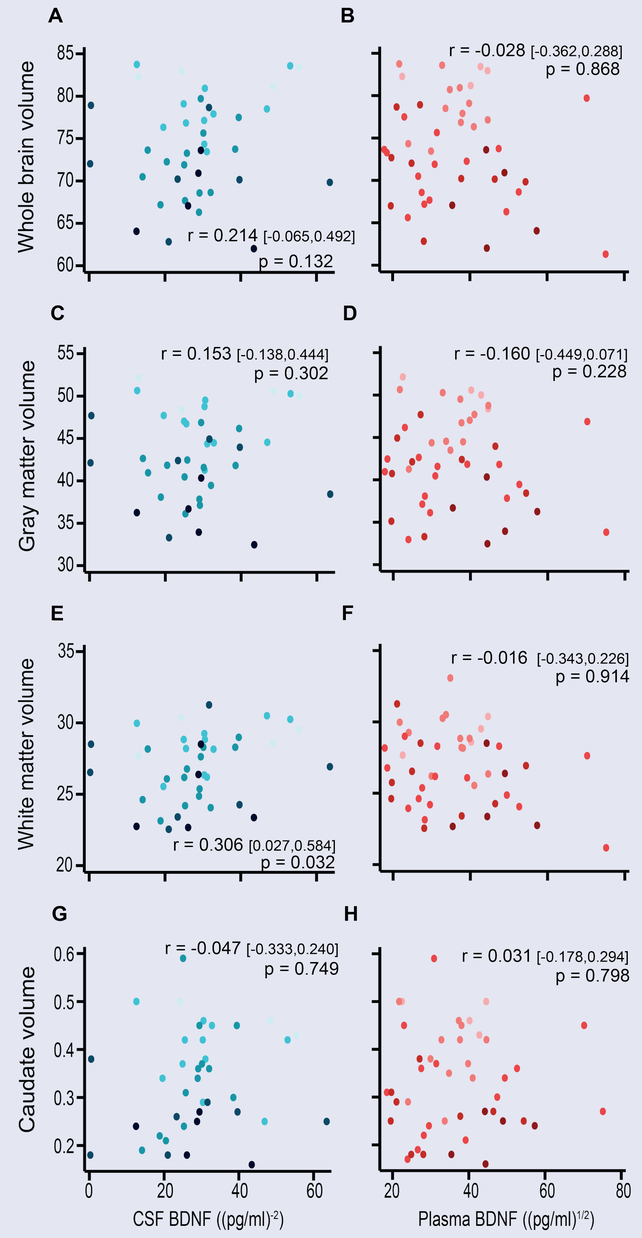

Early preHD | Late preHD | Stage 1 HD | Stage 2 HD | Stage 3 HD

Adjusted correlation coefficient and 95% confidence interval for age, gender, BMI, anti-depressant, anti-psychotic, CAG repeats, storage duration, and platelet level in blood.

Adjusted correlation coefficient and 95% confidence interval for age, gender, BMI, anti-depressant, anti-psychotic, CAG repeats, and erythrocyte level in CSF.

Results: Discriminating ability of BDNF

- Plasma and CSF BDNF showed poor ability to discriminate healthy controls from HD mutation carriers and premanifest HD from manifest HD.

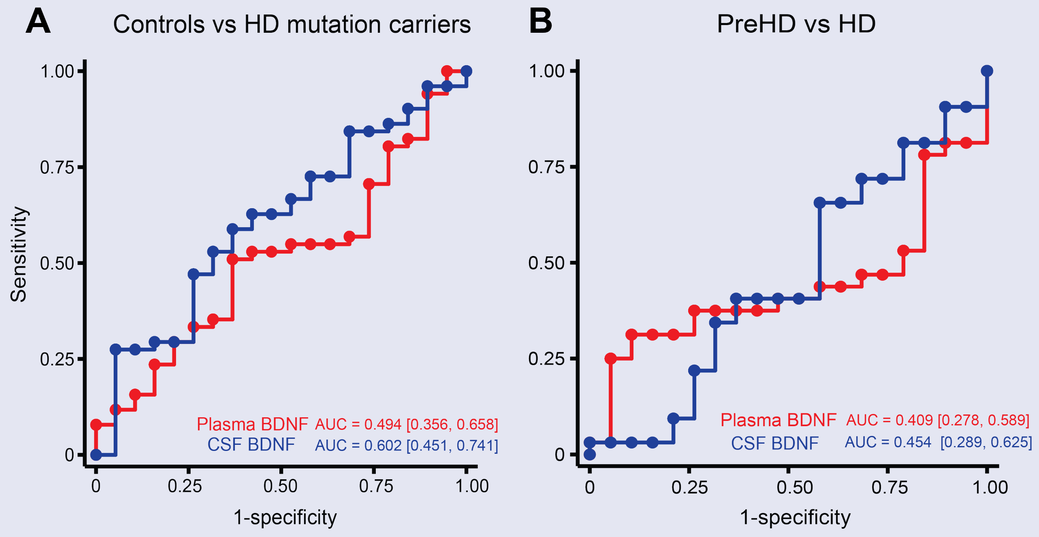

Conclusions

- Unlike the ELISAs, SIMOA is sensitive enough to quantify BDNF in CSF.
- We urge caution in interpreting studies where conventional ELISA was used to quantify CSF BDNF.
- BDNF concentration did not distinguish between the healthy controls and HD mutation carriers at any stage and did not significantly correlate with clinical and imaging measures.
- Based on this data, BDNF does not appear to be a reliable biomarker for Huntington's disease progression.

[1] UCL Huntington's Disease Centre, UCL Queen Square Institute of Neurology, University College London, London, UK.
[2] Lysholm Department of Neuroradiology, National Hospital for Neurology and Neurosurgery, London, UK.
[3] Department of Biomedical Engineering, School of Biomedical Engineering and Imaging Sciences, King's College London, London, UK.
[4] Fluid Biomarker lab, UK Dementia Research Institute at UCL, London, UK.
[5] Department of Psychiatry and Neurochemistry, Institute of Neuroscience and Physiology, Sahlgrenska Academy at the University of Gothenburg, Mölndal, Gothenburg, Sweden.
[6] Clinical Neurochemistry Laboratory, Sahlgrenska University Hospital, Mölndal, Gothenburg, Sweden.

Raised mitochondrial Ca^{2+}; a key determinant in malignant hyperthermia?

Crystal Seng (MD3) and Associate Professor Bradley Launikonis

School of Biomedical Sciences, The University of Queensland, St Lucia, Queensland 4072, Australia

The University Of Queensland

Introduction

Malignant Hyperthermia (MH) is a potentially fatal condition arising upon exposure to volatile anaesthetics

1. It is caused by mutations in the ryanodine receptor (RyR) which induce persistent Ca^{2+} leak into the cytosol of skeletal muscle cells
2. This increases demand on the SERCA pump to hydrolyse ATP in an effort to reduce the raised cytosolic Ca^{2+}
3. It is hypothesised that a portion of this cytosolic Ca^{2+} is taken up by the mitochondria to facilitate ATP generation, yet this would perpetuate the hyperthermic event as this ATP is hydrolysed at the SERCA pump

Here for the first time, we aimed to develop an assay to track and quantify mitochondrial Ca^{2+} and thus provide evidence for mitochondrial involvement in the pathophysiology of MH

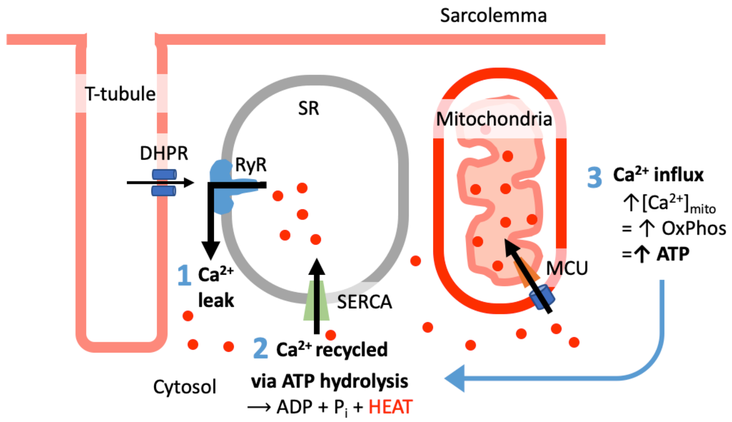

Fig. 1. Schematic of a muscle fibre demonstrating the proposed effect of increased Ca^{2+} leak (red circles) from the RyR on the sarcoplasmic reticulum (SR) and mitochondria in MH.

Methods

The EDL muscles of wild type (C57BL/6J) and mice that were heterozygous or homozygous for the p.G2435R MH mutation were dissected and mechanically skinned. Individual fibres were placed onto a custom-build glass chamber and incubated at 4 °C in a 67 ηM Ca^{2+}-based internal physiological solution containing the fluorescent Ca^{2+} binding dye rhod-2/AM (5 μM) for 10 minutes. Fibres were then imaged with an FV1000 confocal microscope and exposed to 0.25 μM FCCP to quantify mitochondrial $[Ca^{2+}]$.

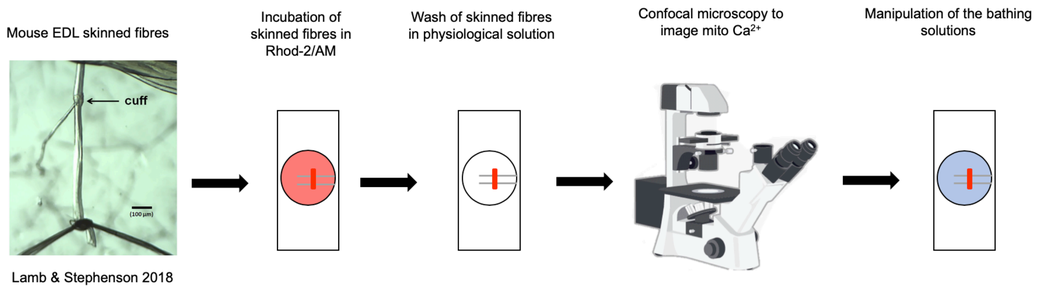

Results

1) Rhod-2 and mitochondrial depolarizing agent FCCP can be used to quantify mitochondrial $[Ca^{2+}]$

- Rhod-2 is a fluorescent dye that binds to mitochondrial Ca^{2+}. Upon addition of FCCP, mitochondrial Ca^{2+} is released allowing a maximum and minimum $[Ca^{2+}]$ to be measured

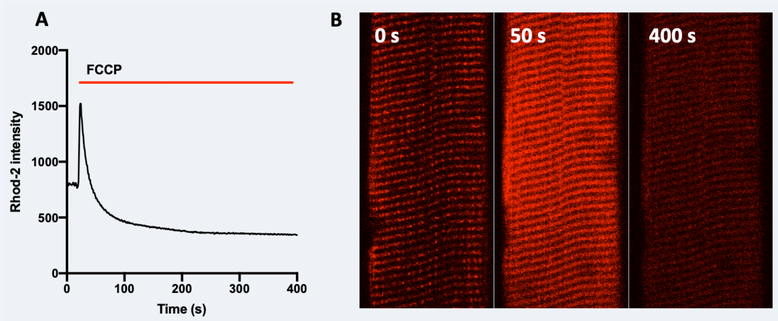

Fig. 2. A) Characteristic trace of an FCCP-induced mitochondrial Ca^{2+} 'spike'
B) Serial xy confocal images before, during and after FCCP addition demonstrating rhod-2 Ca^{2+} fluorescence within mitochondria

2) Mice with an MH mutation have elevated resting mitochondrial Ca^{2+} levels

Fig. 3. Calculated mean resting mitochondrial $[Ca^{2+}]$ across a spectrum of increasing RyR Ca^{2+} leak. Bars show mean + SEM (μM). WT = wild type mice, MH/WT = mice heterozygous for p.G2435R MH mutation, MH/MH = mice homozygous for the mutation. One-way ANOVA demonstrates significance as indicated ($p<0.05$).

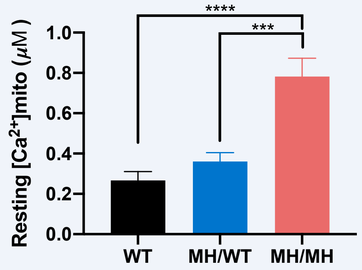

Discussion and Conclusion

- **Increased RyR-Ca^{2+} leak is associated with raised mitochondrial $[Ca^{2+}]$**
- **Mitochondrial $[Ca^{2+}]$ was highest in the homozygous MH mice, which have the leakiest RyR and therefore place the highest demand on SERCA to recycle Ca^{2+}**
- **This implicates the key role of raised mitochondrial Ca^{2+} in perpetuating the hyperthermic event by virtue of a dysregulated physiological process**

References

Santulli G, Xie W, Reiken SR, Marks AR. Mitochondrial calcium overload is a key determinant in heart failure, Proc Natl Acad Sci USA. 2015;112(36):11389-94.
Wescott A, Kao J, Lederer W, Boyman L. Voltage-energized calcium-sensitive ATP production by mitochondria, Nat Metab. 2019;1:975-84.
Williams GS, Boyman L, Chikando AC, Khairallah RJ, Lederer WJ. Mitochondrial calcium uptake. Proc Natl Acad Sci USA. 2013;110(26):10479-86.

Neoantigens Are Typically Associated with Intact HLA Class I Presentation in Early-Stage Follicular Lymphoma

Hennes Tsang[1] , Ann-Marie Patch, PhD[2] , Colm Keane, MD[1,3], Soi C. Law, PhD[1] , Jay Gunawardana, PhD[1] , Piers Blombery, MBBS[4] , Ella R Thompson, PhD, BSc[4] , Muhammed B. Sabdia[1] , Lilia Merida De Long[1] , Clemence J Belle[5] , Karthik Nath, MBBS[1] , Joshua W.D. Tobin, MD[1] , Stephen H Kazakoff, PhD[2] , John F. Seymour[6] , Michael MacManus[7] and Maher K. Gandhi, PhD, FRACP, FRCPath[1,3]

Blood Cancer Research Group, Mater Research Institute, University of Queensland, Brisbane, Australia[1]; QIMR Berghofer Medical Research Institute, Brisbane, Australia[2]; Department of Haematology, Princess Alexandra Hospital, Brisbane, Australia[3]; Department of Pathology, Peter MacCallum Cancer Centre, East Melbourne, Australia[4]; University of Nice, Nice, France[5]; Peter MacCallum Cancer Centre, Melbourne, VIC, Australia[6]; Department of Radiation Oncology, Peter MacCallum Cancer Centre, Melbourne, Australia[7];

Introduction

- Neoantigens are novel peptides created in malignant cells that enable specific antitumour CD8 T-cell immune mediated activity
- We previously demonstrated that high levels of immune infiltration (e.g. CD8 T-cells), was associated with favourable outcomes in advanced-stage Follicular Lymphoma (Tobin, JCO 2019).
- There is minimal data on the immunobiology, frequency and nature of putative neoantigens in early-stage FL (ESFL).
- Characterizing the neoantigen landscape of early-stage Follicular Lymphoma is a key step towards developing novel immunotherapies
- We present detailed characterization of 150 ESFL patients from the TROG99.03 prospective clinical trial (MacManus, JCO 2018).

Methods

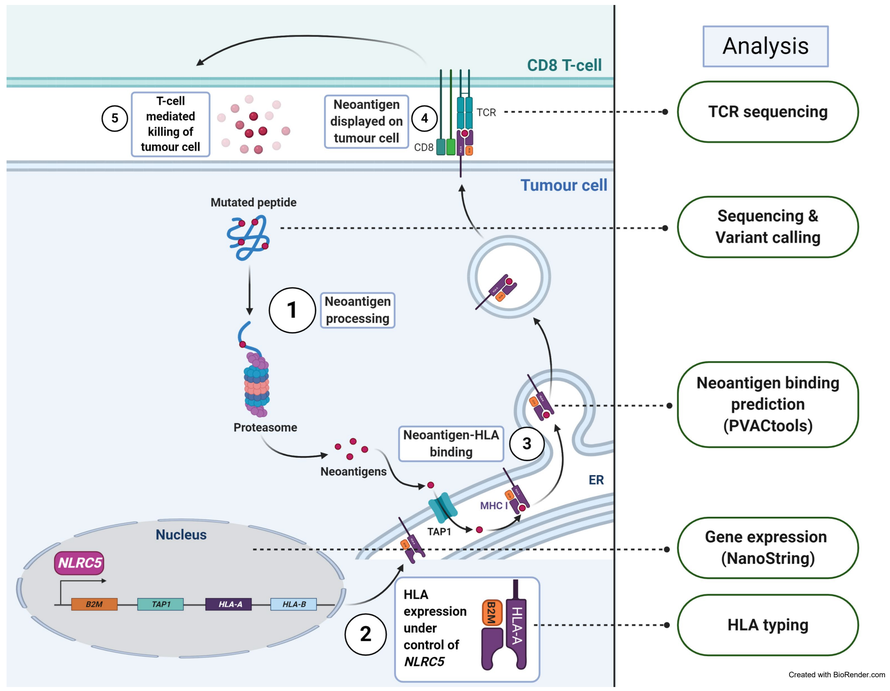

Figure 1. Antitumour CD8 T-cell activity is dependant on neoantigen presentation, a process controlled by *NLRC5* and HLA transcription. Molecular and *in silico* methods may be used to predict the probability of neoantigen presentation.

NanoString Digital gene expression (770 genes) and targeted sequencing (365 genes) were performed on tumour samples. HLA genotyping was performed by custom NGS panel on germline blood. Neoantigen binding effectiveness was estimated using eight algorithms with PVACtools (Hundal, CIR 2020). Neoantigens were defined as having a half maximal inhibitory concentration (IC50) score of <50 (high affinity binding to HLA groove), and fold-change of >1 (mutant peptide binds more than wild-type peptide).

Results

High expression of *CD8A*, marker of cytotoxic T-cells, and *NLRC5*, transcriptional regulator of HLA, associated with favourable outcomes

High intra-tumoral *CD8A* expression was associated with >2-fold differential median progression free survival (PFS) (*CD8A*^{Hi}: 11.5 years vs. *CD8A*^{Lo}: 4.9 years, p=0.0042, Figure 2 A.). *NLRC5* expression was also associated with differential median PFS (*NLRC5*^{Hi}: 10.8 years vs. *NLRC5*^{Lo}: 4.9 years, p=0.021, Figure 2 B.)

Samples with neoantigens are associated with intact HLA expression

Unsupervised hierarchical clustering showed 2-fold enrichment of samples with neoantigens and elevated HLA A/B expression (p=0.0023, Figure 2 C.).

2A. PFS by *CD8A* levels

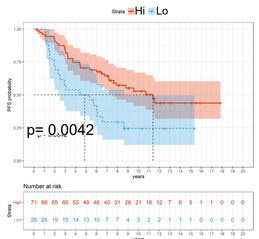

2B. PFS by *NLRC5* levels

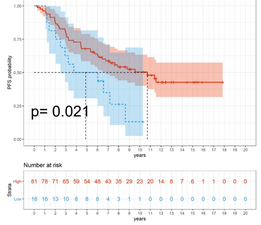

2C. Heatmap of HLA related genes labelled by samples with neoantigens

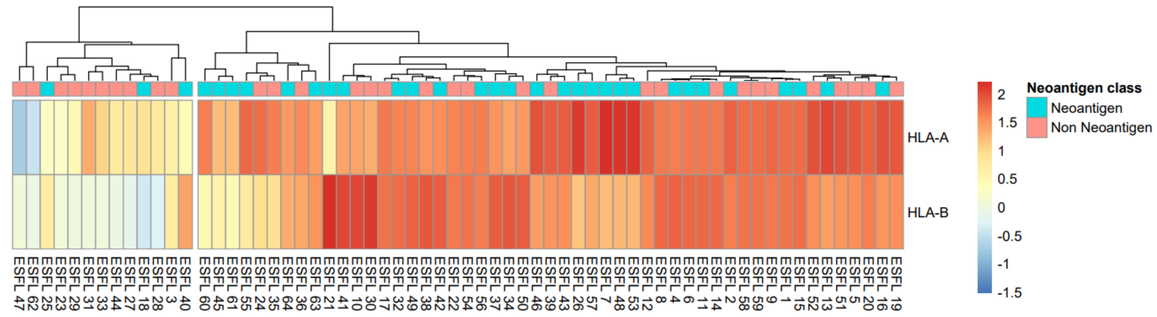

Figure 2. A) Progression free survival (PFS) Kaplan-Meier estimates of patients from the TROG99.03 prospective clinical trial categorized by high and low expression of CD8A. **B)** PFS estimates categorized by high and low expression of *NLRC5*. **C)** Heatmap stratified by immune infiltration (*PD-L2, CD8A*) and genes involved in antigen processing (*TAP1/2, PSMB8/9, NLRC5*), of HLA A/B gene expression in ESFL diagnostic tissue samples. Samples with putative neoantigens are shown in blue, and non-neoantigens in pink. 77% of the HLA A/B low clade (left) contains non-neoantigens.

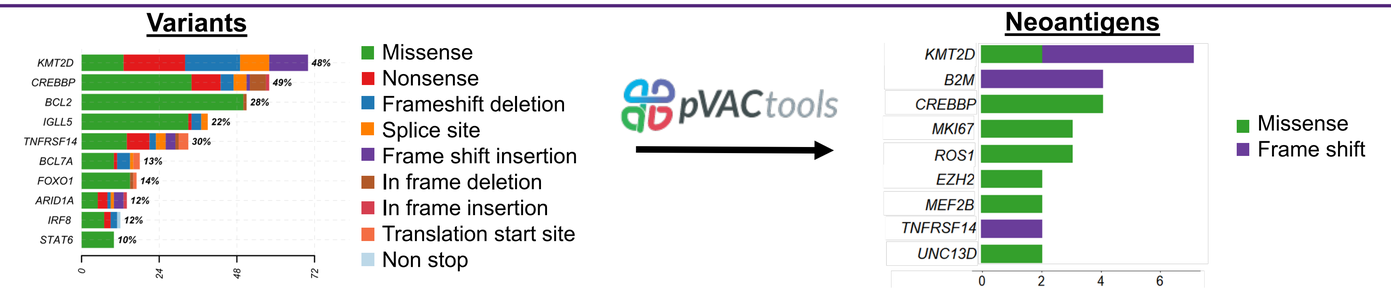

Figure 3. Variants called from the TROG99.03 ESFL cohort were processed with pVACtools for neoantigen prediction. The most mutated gene, *KMT2D*, resulted in the most number of predicted neoantigens of which a majority were derived from frame shift mutations.

KMT2D was the most mutated gene and had the most predicted neoantigens

Frameshift mutations that may result in immunogenic neo open reading frame peptides (NOPs) were the most frequently detected neoantigen type in the highly mutated gene *KMT2D* (Figure 3).

Conclusions

We demonstrate for the first time in ESFL that neoantigens are associated with intact HLA class I presentation; CD8 infiltration is associated with neoantigen processing and favourable outcomes; a subset of FL tumours has potential immunogenic NOPs from the highly mutated gene *KMT2D*. These data will inform the design of personalized next-generation immunotherapy for FL.